Since January 2020 Elsevier has created a COVID-19 resource centre with free information in English and Mandarin on the novel coronavirus COVID-19. The COVID-19 resource centre is hosted on Elsevier Connect, the company's public news and information website.

Diagnostic Microbiology and Infectious Disease 79 (2014) 432–437

Contents lists available at ScienceDirect

Diagnostic Microbiology and Infectious Disease

journal homepage: www.elsevier.com/locate/diagmicrobio

Mycobacteriology

A proteomics approach to the identification of plasma biomarkers for latent tuberculosis infection

Xia Zhang, Fei Liu, Qi Li, Hongyan Jia, Liping Pan, Aiying Xing, Shaofa Xu *, Zongde Zhang **

Department of Beijing Key Laboratory of Drug Resistance Tuberculosis Research, Beijing Chest Hospital, Capital Medical University, Beijing Tuberculosis and Thoracic Tumor Research Institute, Beijing, China

ARTICLE INFO

Article history:
Received 6 December 2013
Received in revised form 18 April 2014
Accepted 21 April 2014
Available online 26 April 2014

Keywords:
Latent tuberculosis infection
Proteomics
Plasma
MALDI-TOF-MS

ABSTRACT

A proteomic analysis was performed to screen the potential latent tuberculosis infection (LTBI) biomarkers. A training set of spectra was used to generate diagnostic models, and a blind testing set was used to determine the accuracy of the models. Candidate peptides were identified using nano-liquid chromatography-electrospray ionization–tandem mass spectrometry. Based on the training set results, 3 diagnostic models recognized LTBI subjects with good cross-validation accuracy. In the blind testing set, LTBI subjects could be identified with sensitivities and specificities of 85.20% to 88.90% and 85.7% to 100%, respectively. Additionally, 14 potential LTBI biomarkers were identified, and all proteins were identified for the first time through proteomics in the plasma of healthy, latently infected individuals. In all, proteomic pattern analyses can increase the accuracy of LTBI diagnosis, and the data presented here provide novel insights into potential mechanisms involved in LTBI.

1. Introduction

Tuberculosis (TB) is a major cause of mortality worldwide, causing an estimated 1.7 million deaths each year, and the global number of new cases (more than 9 million) is higher than at any other time in history (Lawn and Zumla, 2011). Most people infected with *Mycobacterium tuberculosis* (MTB) retain the initial infection and develop latent TB. This state is characterized by evidence of an immune response against the bacterium but no signs of active infection. Latent TB can be maintained for the lifetime of the infected person. However, the MTB bacilli that persist in symptom-free individuals can reactivate and cause active disease in approximately 10% of those infected over a lifetime (Jasmer et al., 2002; Pai et al., 2004; Tufariello et al., 2003). An estimated one-third of the world's population is infected with MTB (Dye et al., 1999). This large reservoir of individuals with latent TB infection (LTBI) poses a hurdle for TB elimination (CDC, 2000; Sterling et al., 2006, 2011).

For nearly a century, the tuberculin skin test (TST) was the only available test for the detection of LTBI. However, the TST has its limitations, including low sensitivity in immunocompromised patients, cross-reactivity with the Bacille Calmette-Guérin vaccine and environmental mycobacteria, and the need for a second visit, which often results in missed follow-ups (Menzies, 2000). A decade ago, interferon-γ release assays (IGRAs) were developed, in which interferon-γ titres are measured after the in-vitro stimulation of peripheral blood mononuclear cells with antigens such as early secreted antigenic target 6 (ESAT-6) and culture filtrate protein 10 (CFP-10). IGRAs have now become the gold standard for identifying individuals whose immune systems have previously encountered MTB (Lawn and Zumla, 2011). However, the sensitivity of these assays remains limited (70–85%) (Sester et al., 2011), and the higher material costs of IGRAs and their need for laboratory infrastructure, trained personnel, and venipuncture under field conditions pose serious practical limitations, particularly for high-burden, resource-limited countries. To date, no community-based surveys have been performed using IGRAs. In addition, the mechanisms involved in maintaining a latent infection are complex, and many fundamental questions regarding these mechanisms remain unanswered. Consequently, there is a need for better biomarkers for diagnosing LTBI and a greater understanding of the LTBI pathogenesis.

The discovery of biomarkers in body fluids has been advanced by the development of high-throughput spectrometric methods (Faulkner et al., 2012; Fertin et al., 2011). Particularly, magnetic beads combined with matrix-assisted laser desorption/ionization time-of-flight mass spectrometry (MALDI-TOF MS) are a promising high-throughput approach to identify new potential biomarkers in various body fluids. Magnetic beads have large surface area and can capture more low-abundance peptides and proteins. The combination of magnetic beads and MALDI-TOF MS can leverage the advantages of both methods and, therefore, reduce the complexity and enrich low-abundance proteins (Huang et al., 2009). The technical performance of affinity bead purification is similar to that of enzyme-linked immunosorbent assay, and it can be used to process many samples in parallel (Cheng et al., 2005). Many protein biomarkers of diseases have been identified using

* Corresponding author. Tel.: +86-10-89509155; fax: +86-10-69546819.
** Corresponding author. Tel.: +86-10-89509365; fax: +86-10-69546819.
E-mail addresses: shaofaxu8950@126.com (S. Xu), zhang2001512@126.com (Z. Zhang).

http://dx.doi.org/10.1016/j.diagmicrobio.2014.04.005
0732-8893/

this technique (Dekker et al., 2010; Fiedler et al., 2009; Komori et al., 2012; Schwamborn et al., 2009). Previously, 1 study demonstrated that proteomic patterns based on such profiles can distinguish active TB from non-TB individuals (Deng et al., 2011). However, there remains a lack of published data using this method as a tool for biomarker discovery in LTBI.

In this study, we applied magnetic beads combined with MALDI-TOF MS to analyze plasma samples from healthy, latently infected individuals and healthy, MTB-noninfected controls for infection-associated biomarkers, with the aim of determining the diagnostic accuracy of these putative peptide biomarkers and better understanding the LTBI pathogenesis.

2. Materials and methods

2.1. Study design and population

The study was conducted according to the principles of the Declaration of Helsinki and approved by the ethical committees of Capital Medical University/Beijing Chest Hospital. All participants were at least 18 years old, HIV negative, and provided written, informed consent. Subjects were prospectively enrolled and recruited from the staff at Beijing Chest Hospital, Capital Medical University, China, between June and October 2012. Healthy, latently infected subjects were recruited from close contacts of active TB patients and had positive TST and T-SPOT.TB tests, normal chest computed tomography (CT), no clinical symptoms or evidence of active TB, and no clinical evidence of the other diseases, such as other non-tuberculous respiratory infections and lung cancer (Lu et al., 2011; Shao et al., 2008). Healthy MTB-noninfected controls were recruited from people with no exposure to MTB, negative TST and T-SPOT.TB tests, normal chest CT, and no clinical evidence of diseases. Individuals were excluded if they had a prior history of TB or another infectious disease, if they had a history of diabetes, if they were hepatitis B virus (HBV) positive or hepatitis C virus (HCV) positive (these 2 diseases are highly prevalent in China), or if they refused or were unable to give consent.

During the course of the study, 86 healthy participants with LTBI and 77 healthy participants with no TB infection (controls) were enrolled. Of these participants, 17 were excluded from the study for the following reasons: a history of TB or another infectious disease (n = 12), HBV- or HCV-positive individuals (n = 2), or a history of diabetes (n = 3). The final study samples comprised 146 subjects, of which 71 were from individuals with LTBI and 75 from healthy controls.

We analyzed the peptidome fingerprints of the training set (44 LTBI individuals and 47 healthy controls) for the model generation and designated 27 LTBI individuals and 28 healthy controls as the blind testing set for validation (Fig. 1). The demographic features of the training and blind testing sets are summarized in Table 1.

2.2. Clinical assessment and definition of LTBI

All participants underwent a standardized interview, a physical examination, a chest CT, sputum smear, a TST, testing for 1 commercial IGRA — the T-SPOT.TB test (Oxford Immunotech, Oxford, UK), a complete blood count, and the Abbott AxSYM anti-HBsAg and HCV 3.0 antibody assay kit (Abbott Laboratories, Chicago, IL, USA).

A diagnosis of LTBI was defined in accordance with guidelines from the National Institute for Health and Clinical Excellence (National Institute for Health and Clinical Excellence, 2011): close contacts with active TB, positive TST, and T-SPOT.TB tests in the absence of clinical and radiological and microbiological evidence for active TB. A team of 2 TB physicians and 2 radiologists reviewed all available medical records. When there was disagreement regarding the diagnosis, a

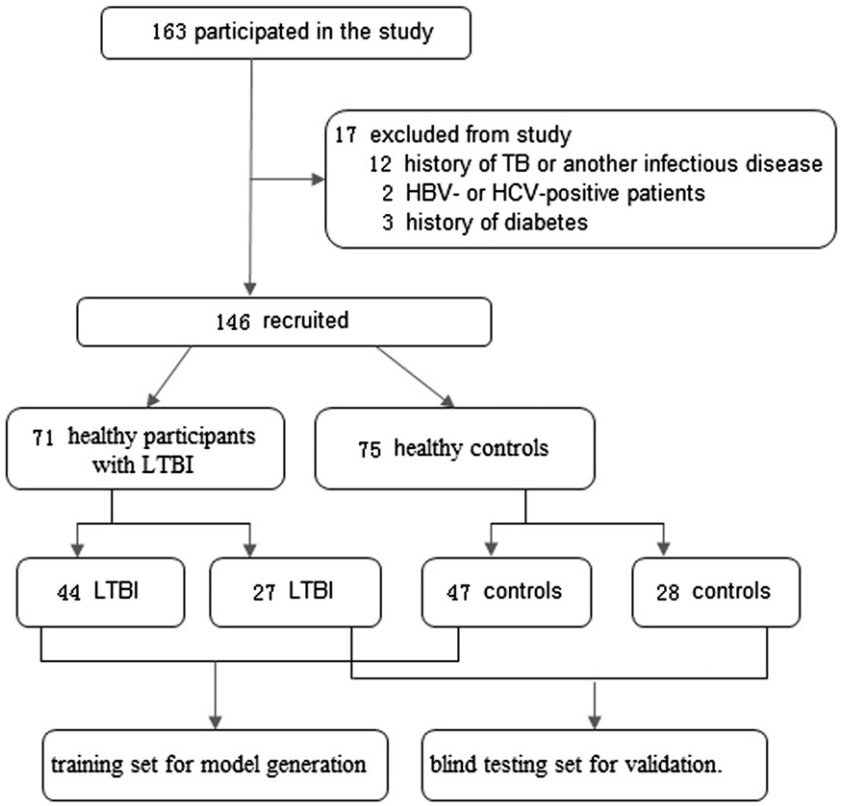

Fig. 1. Screening and enrollment of the study participants. Of 163 participants, 17 individuals were excluded. The final study sample comprised 146 subjects, of which 71 were individuals with LTBI and 75 were healthy controls. The LTBI individuals and the healthy controls were subdivided into a training set (44 LTBI individuals and 47 healthy controls) for model generation and a blind testing set (27 LTBI individuals and 28 healthy controls) for validation.

Table 1
Demographics of the study participants.

Study complex	Variables	LTBI	Controls	*P* value
Training set				
	n	44	47	
	Male/female	21/23	23/24	0.442
	Mean age ± SD (y)	42.9 ± 9.4	43.8 ± 8.3	0.647
	Age range (y)	22-58	29-58	
	Mean BMI ± SD	24.8 ± 3.0	23.7 ± 2.5	0.055
	Smokers/nonsmokers	10/34	14/33	0.445
Blind testing set				
	n	27	28	
	Male/female	9/18	10/18	0.853
	Mean age ± SD (y)	41.1 ± 8.4	41.3 ± 9.0	0.941
	Age range (y)	23-56	23-62	
	Mean BMI ± SD	23.4 ± 2.6	24.5 ± 1.9	0.073
	Smokers/Nonsmokers	4/23	4/24	0.956

n = numbers of participants; SD = standard deviation; y = years; BMI = body mass index.

third physician or radiologist refereed. The radiologists were blinded to the results of the other tests.

2.3. Blood sample collection

All samples were collected and processed according to a feasible and highly standardized preanalytical protocol (Baumann et al., 2005). We collected 3 mL of heparinized plasma from each participant. To obtain fresh plasma, we centrifuged the blood specimens at 1400 g for 10 min at room temperature within 4 h of collection. The plasma was then aliquoted into 1.5 mL polypropylene tubes for immediate freezing at −80 °C. All samples avoided freeze-thawing cycles.

2.4. Tuberculin skin test

As recommended by the World Health Organization standard Mantoux technique (WHO, 1963), the TST was administered by trained nurses using 0.1 mL (2 tuberculin units) of purified protein derivative RT 23 (Statens Serum Institute, Copenhagen, Denmark). The test was read 72 h later using 10-mm diameter as the cut-off point. To reduce variations in reading, double-blind reading was performed by 2 independent readers, using the average measures in the analysis. Blood for T-SPOT.TB test was collected before TST application.

2.5. T-SPOT.TB test

The T-SPOT.TB test was performed according to the manufacturer's instructions (Oxford Immunotec, Oxford, UK). Peripheral blood mononuclear cells (PBMCs) were isolated by centrifugation, washed twice, and re-suspended in GIBCO AIM-V (Invitrogen, Auckland, New Zealand). PBMCs were stimulated with ESAT-6 and CFP-10 in 96-well plates and incubated overnight at 37 °C in 5% CO_2. After the incubation, wells were washed 4 times with phosphate buffer solution and incubated for 1 h at 2–8 °C with a monoclonal antibody to interferon-γ conjugated with alkaline-phosphatase. After washing 4 more times and adding a chromogenic substrate, the presence of reactive antigen-specific T cells was revealed as a spot on the well. Automated spot counting was performed using a 166 CTL ELISPOT system (CTL-ImmunoSpot® S5 Versa Analyzer, Cleveland, OH, USA). The results were recorded based on the definition of positive and negative reactions given in the instructions from the manufacturer. Responses were scored positive if the test wells contained a mean of at least 6 spot-forming cells more than the mean of the negative control wells and if this number was at least twice the mean of the negative control wells.

2.6. Magnetic beads fractionation and MALDI-TOF MS analysis

All samples were fractionated using weak cation exchange magnetic beads (MB-WCX) according to the manufacturer's recommendations (Bruker Daltonics, Bremen, Germany). Briefly, the suspension in the magnetic bead was mixed by shaking. After eluting and beating, the MB-WCX were separated from the protein, and the eluted peptide samples were transferred to a 0.5-mL clean sample tube for further MS analysis. Five microliters of alpha-cyano-4-hydroxycinnamic acid substrate solution (0.4 g/L, dissolved in acetone and ethanol) and 0.8–1.2 μL of elution were mixed. Next, 0.8–1.2 μL of this mixture was applied to a metal target plate and dried at room temperature. Finally, the prepared sample was analyzed by MALDI-TOF MS (Bruker Daltonics). A range of 1000–10,000 Da peptide molecular weights was collected, and 400 shots of laser energy were used.

To evaluate the precision of the assay, within-run and between-run variations were determined using multiple analyses of the bead fractionation and MS for 2 plasma samples. To assess within-run variability, each plasma sample was loaded onto 3 spots. To assess between-run variability, identical samples were assayed 3 times independently. In each profile, 3 peaks with different molecular masses were selected to evaluate the within-run and between-run coefficients of variance (CV).

2.7. Identification of differentially expressed candidate biomarkers

The peptides from plasma samples were eluted from the magnetic beads and analyzed by nano-liquid chromatography–electrospray ionization–tandem mass spectrometry (nano-LC/ESI–MS/MS) system consisting of an Aquity UPLC system (Waters) and a linear ion trap quadrupole (LTQ) Obitrap XL mass spectrometer (Thermo Fisher) equipped with a nano-ESI source. The peptides were loaded to a C18 trap column (nanoACQUITY) [180 μm × 20 mm × 5 μm (symmetry)]. The flow rate was 15 μL/min. The desalted peptides were then analyzed by a C18 analytical column (nanoACQUITY) [75 μm × 150 mm × 3.5 μm (symmetry)] at a flow rate of 400 nL/min. The mobile phases A (5% acetonitrile, 0.1% formic acid) and B (95% acetonitrile, 0.1% formic acid) were used for analytical columns. The gradient elution profile was as follows: 5%B-50%B-80%B-80%B-5%B-5%B in 100 min. The MS instrument was operated in a data-dependent model. The range of the full scan was 400–2000 Da with a mass resolution of 100,000. The 8 most intense monoisotope ions were used as the precursors for a collision-induced dissociation.

2.8. Western blot analysis

Samples were run on 12% sodium dodecyl sulfate–polyacrylamide gels and transferred onto polyvinylidene difluoride membranes (Millipore Corporation, Billerica, MA, USA) by electroblotting and then blocked for 1 h with Tris-buffered saline-T buffer (10 mmol/L Tris-HCl, 150 mmol/L NaCl, 0.1% Tween 20 containing 5% skim milk). The primary antibodies used were rabbit anti-fibrinogen alpha chain antibody (diluted 1:4000, Abcam, Cambridge, MA, USA), mouse anti-Transketolase antibody (diluted 1:1000, Abcam), rabbit anti-Peroxiredoxin-I antibody (diluted 1000, Abcam), rabbit anti-ubiquitin-like modifier activating enzyme 1 (diluted 1:1000; Abcam), rabbit anti-T-complex protein 1 subunit beta antibody (diluted 1:1000; Abcam), rabbit anti-Myosin-9 antibody (diluted 1:2000; Abcam). Membranes were incubated at room temperature for 1 h with each primary antibody and then were washed 3 times and incubated with horseradish peroxidase-conjugated anti-rabbit IgG (diluted 1:20000; Santa Cruz Biotechnology, Santa Cruz, CA, USA) or anti-mouse IgG (diluted 1:10000, Santa Cruz Biotechnology) for 1 h at room temperature. The reactions were detected by chemiluminescence with an electrochemiluminescence kit (Amersham Biosciences, Buckinghamshire, UK) as recommended by the manufacturer. Proteins levels were

Table 2
Peak selection of the algorithm models.

Algorithm	Peak selection (*m/z*)
SNN	2662, 2212, 1452, 4969, 4988, 2864, 2645, 2683, 2700, 1995, 2487, 2008, 8785, 5910, 8944, 2085, 1084, 1074, 2792
QC	2662
GA	2662, 1898, 2962, 1052, 1982

normalized using Ponceau S staining of the membranes used as the loading control. The density of each band was measured with TotalLab Quant software (TotalLab, Newcastle, UK).

2.9. Statistical analysis

The resulting spectra were analyzed using ClinProTools (ClinProt software version 2.0; Bruker Daltonics). Peaks of interest were selected from the total average spectra using a signal-to-noise threshold of 5. To align the spectra, a mass shift of no more than 0.1% was determined. After each profile was generated, a 20% leave out cross-validation process was performed within the software. The comparison of relative peak intensity levels between classes was also calculated within the software suite. Student's *t* test was used to analyze normally distributed continuous data, whereas the Wilcoxon test was used for non-normally distributed continuous data. A Chi-square test was used for the categorical data analysis. $P < 0.05$ was considered statistically significant. Genetic algorithm (GA), supervised neural network (SNN), and quick classifier (QC) algorithms contained in this software suite were used to establish models for identifying LTBI individuals from healthy controls. Models performed on the training set were then validated on the blind testing set. The receiver operating characteristic (ROC) curve and area under the curve (AUC) analyses were used to determine the diagnostic efficacy of each single marker and each model.

3. Results

3.1. Peptides analysis

Over the mass range analyzed (1000–10,000 Da), 66 peptides were detected at a signal-to-noise threshold of 5, of which 5 peaks were significantly different between LTBI individuals and healthy controls ($P < 0.05$). Preliminary statistical analysis was performed for these 5 peaks by ROC analysis. AUC of peak 1 at mass-to-charge ratio (*m/z*) 2662, of peak 2 at *m/z* 2645, and of peak 3 at *m/z* 2683 were 1.000 (95% confidence interval [CI] 0.959–1.000), 0.936 (95% CI 0.865–0.977), and 0.915 (95% CI 0.838–0.964), respectively, which corresponds to a highly accurate test. AUC of peak 4 at *m/z* 2700 and of peak 5 at *m/z* 1995 were 0.795 (95% CI 0.698–0.873) and 0.692 (95% CI 0.586–0.784), respectively, which corresponds to a moderately accurate test. These 5 peaks and their ROC, *P* values, and AUC values are depicted separately in Fig. S1. The overall spectra of LTBI individuals and healthy controls are displayed in Fig. S2, showing protein profiles from 1 to 10 kDa.

To determine the precision of the assay, the within-run and between-run reproducibility of 2 samples was evaluated with the data. CVs from within-run and between-run assays are summarized in Table S1 in the online data supplement. The mean CVs of the runs represent the overall imprecision, <8% in the within-run and between-run assays, indicating that the results produced by this method were highly reproducible.

3.2. Model building and blind test

In the training set, 3 different classification models for LTBI individuals and healthy controls were generated using GA, SNN, and QC algorithms. The use of pairs of peaks yielded the best performances. The GA, SNN, and QC models performed reasonably well on the training set to discriminate control and LTBI samples, with cross-validation accuracies and recognition capabilities of 89.8% and 94.5%, 89.5% and 100.0%, and 94.2% and 91.1%, respectively. Peaks selected by these 3 models are provided in Table 2.

To assess the accuracy and validity of the classification models derived from the training set, we applied the models to the blind testing set consisting of 27 LTBI individuals and 28 healthy controls. The 3 models also performed well on the testing set, with sensitivities of 85.2%–88.9% and specificities of 85.7%–100.0% (Table 3). In the ROC analysis of the GA, SNN, and QC models, AUC of the 3 models in the training set and blind testing set were 1.000 (95% CI 0.960–1.000), 1.000 (95% CI 0.960–1.000), 1.000 (95% CI 0.959–1.000), and 0.991 (95% CI 0.918–1.000), 1.000 (95% CI 0.935–1.000), 0.974 (95% CI 0.890–0.998), respectively, which corresponds to a highly accurate test, suggesting that LTBI individuals and healthy controls were well-discriminated by these models (Fig. S3).

3.3. Identification of the LTBI biomarkers

To identify the peptides observed in the MS profiles as possible biomarkers of LTBI, we attempted to identify as many of the detected peaks as possible. Peaks in the GA, SNN, and QC models were selected for protein identification. Using LTQ-Orbitrap-MS detection, 14 of the 23 differentially expressed peptides were successfully identified (Table 4).

3.4. Validations by Western blot analysis

To validate the results of our study, Western blots were used to examine the expression of peroxiredoxin-I (Prx-I), myosin-9 (MYH9), transketolase (TKT), fibrinogen alpha chain (FGA), ubiquitin-like modifier activating enzyme 1 (UBA1), and t-complex protein 1 subunit beta (CCT2). As shown in Fig. S4, for the 6 proteins, the Western blot results showed the same pattern of expression as that obtained from proteomic data. Significantly higher levels of MYH9 ($P = 0.028$), TKT ($P = 0.011$), FGA ($P = 0.002$), and UBA1 ($P = 0.048$) were found in LTBI individuals when compared to healthy controls. Lower levels of Prx-I ($P = 0.026$) and CCT2 ($P = 0.073$) were found in LTBI individuals when compared to healthy controls, but CCT2 was not statistically significant.

Table 3
Algorithm for separation of healthy participants with LTBI and healthy controls.

Algorithm	Sensitivity, %	Specificity, %	Accuracy, %	Positive predictive value, %	Negative predictive value, %
	95% CI, %	95% CI, %	95% CI, %	95% CI, %	95% CI, %
SNN	88.9	96.4	92.7	96.0	90.0
	77.1–100.0	89.5–100.0	85.8–99.6	88.3–100.0	79.3–100.0
QC	85.2	100.0	92.7	100.0	87.5
	71.8–98.6	100.0–100.0	85.8–99.6	100.0–100.0	75.0–99.0
GA	85.2	85.7	85.5	85.2	85.7
	71.8–98.6	72.7–98.7	76.2–94.8	71.8–98.6	72.7–98.7

Table 4
List of identified proteins.

m/z	Protein ID	Protein description	Protein symbol	Peptides sequence	Expression
2662	IPI100021885.1	Fibrinogen alpha chain precursor	FGA	A.DEAGSEADHEGTHSTKRGHAKSRPV.R	Up
2645	IPI00643920.2	Transketolase	TKT	K.SKDDQVTVIGAGVTLHEALAAAELLK.K	Up
2700	IPI00180240.2	Thymosin beta-4-like protein 3	TMSL3	K.TETQEKNPLPSKETIEQEKQAGES.-	Up
1995	IPI00021857.1	Apolipoprotein C-III precursor	APOC-III	F.SEFWDLDPEVRPTSAVAA.-	Down
4988	IPI00304273.2	Apolipoprotein A-IV precursor	APOA-IV	F.FSTFKEKESQDKTLSLPELEQQQEQQQEQQQEQVQMLAPLES.-	Down
1982	IPI00000874.1	Peroxiredoxin-I	Prx-I	R.TIAQDYGVLKADEGISFR.G	Down
1052	IPI00218192.2	Inter-alpha-trypsin inhibitor heavy chain H4 precursor	ITIH4	G.SEMVVAGKLQ.D	Down
2962	IPI00021841.1	Apolipoprotein A-I precursor	APOA-I	D.NWDSVTSTFSKLREQLGPVTQEFWD.N	Down
2683	IPI00026119.6	Ubiquitin-like modifier activating enzyme 1	UBA1	K.IHVSDQELQSANASVDDSRLEELK.A	Up
1452	IPI00739237.1	Similar to complement component 3	LOC653879	I.THRIHWESASLL.R	Up
2487	IPI00076042.2	Short heat shock protein 60	Hsp60	R.TALLDAAGVASLLTTAEVVVTEIPK.E	Down
2008	IPI00297779.7	T-complex protein 1 subunit beta	CCT2	R.EGTIGDMAILGITESFQVK.R	Down
2085	IPI00292657.3	NADP-dependent leukotriene B4 12-hydroxydehydrogenase	LTB4DH	K.GGETVMVNAAAGAVGSVVGQIAK.L	Up
2792	IPI00019502.3	Myosin-9	MYH9	K.SGFEPASLKEEVGEEAIVELVENGKK.V	Up

4. Discussion

In this study, we demonstrated that magnetic beads in combination with MALDI-TOF MS could differentiate healthy, latently infected individuals from healthy MTB-noninfected controls with high sensitivity and specificity (>85%). ClinProt is a well-established system that enables proteomic profiling using the bioinformatics software ClinProTools, which provides algorithms for multivariate statistical analyses and improves the detection of candidate peaks (Ishigami et al., 2012). In 2012, Sandhu et al. (2012) published a report demonstrating that active TB can be accurately distinguished from LTBI in symptomatic patients using surface-enhanced laser desorption/ionization time-of-flight mass spectrometry (SELDI-TOF-MS). Unfortunately, this research did not identify the distinguishing proteins because the major drawback of the SELDI-TOF-MS approach is that the retained proteins cannot be directly recovered from the ProteinChip arrays. Moreover, chip-to-chip variation is another obstacle for the SELDI analysis. To overcome these problems, a magnetic bead-based plasma profiling method was developed in this study. This method leaves sufficient materials for subsequent protein identification experiments and can reduce assay-to-assay and researcher-to-researcher variations using functionalized magnetic beads and automated machines (Wong et al., 2010).

Our study identified 14 plasma proteins in subjects with LTBI by nano-LC/ESI–MS/MS. Compared with healthy controls, 7 proteins were up-regulated, and 7 proteins were down-regulated in LTBI individuals. To our knowledge, all proteins were identified for the first time through proteomics in the plasma of healthy, latently infected individuals. Selected descriptions of the proteins that may be involved in the LTBI pathogenesis are discussed as follows.

We have found many acute phase proteins (APPs) in the plasma of subjects with LTBI. These proteins may take part in inflammation control, which implicates active innate immune responses in an infection with MTB and suggests that the inflammatory response may play an important role during an LTBI. Among the APPs found in LTBI, fibrinogen is a necessary cofactor for toxic and proinflammatory activities. Fibrinogen includes fragments of the fibrinogen α, β, and γ chains, but in this study, we demonstrate that the fibrinogen α chain precursor is the best discriminator and GA, SNN, and QC these 3 models all selected this protein. It is possible that fibrinogen α chain is more associated with an inflammatory response to MTB than β and γ chains of fibrinogen. Liu et al. (2008) found that fibrinogen was up-regulated in the proteomic profiling of TB pericardial effusions and proposed that fibrinogen may be significantly involved in the etiology of the tuberculous pericardial effusion. A study of an in vivo mice model of mycobacterial granuloma formation observed that fibrinogen promoted granulation tissue formation and suppressed leukocyte necrosis (Sakamoto et al., 2010). In the present study, we found that the fibrinogen α chain precursor was significantly increased in the plasma of LTBI individuals. Our results and those of other investigators indicate that fibrinogen and/or its fragments may be involved in the pathophysiologic mechanisms of TB or LTBI and may serve as useful markers.

Inter-alpha-trypsin inhibitor heavy chain H4 (ITIH4) is another positive APP that is related to cell proliferation and migration during the development of the acute-phase response and involved in infection and inflammation. In previous studies, ITIH4 was a positive marker in proteomic fingerprinting studies of chronic obstructive pulmonary disease (Bandow et al., 2008) and dairy calves with experimentally induced pneumonia (Piñeiro et al., 2004).

Apolipoprotein A-I (ApoA-I) belongs to the negative APPs that play major roles in the transport of nutrients, hormones, and metabolites. ApoA-I is a major component of high-density lipoproteins. A decline in high-density lipoproteins renders the host tissue more susceptible to bacterial substance-mediated injury, resulting in cytokine overproduction and a further depletion of high density lipoprotein (vicious cycle) (Chien et al., 2005). ApoA-I has been demonstrated to be a negative marker in severe acute respiratory syndrome (Wan et al., 2006). It is unclear why this protein was down-regulated in LTBI. Mikkat et al. (2004) have shown that the concentrations of some negative APPs decrease in response to infection and inflammation because of increased transcapillary escape and catabolic rates.

For decades, although the productions of APPs are not agent-specific, their levels of expression have been used as biological markers of tissue injury and of the onset and progression of a variety of disease processes (Endeman et al., 2011; Martìnez Cordero et al., 2008). The APPs are generated as a systemic response not only to acute inflammatory stimuli but also to chronic inflammation. Thus, we can utilize our identified APPs as markers to predict active TB and other inflammatory diseases, but further studies and including active TB and other inflammatory diseases into the studies are needed to confirm this prediction.

Immune responses to MTB drive the bacteria into a latent state. UBA1, which was up-regulated in LTBI individuals, mediates the human HLA-F adjacent transcript 10 (FAT10) modification that is significantly involved in the immune response (Aichem et al., 2010). HLA-F adjacent transcript 10 expression is induced by interferon-γ and tissue necrosis factor α, which are crucial for protective immunity against mycobacteria (Tufariello et al., 2003). Another up-regulated enzyme, leukotriene B4 12-hydroxydehydrogenase (LTB4DH), is a member of the zinc-independent medium chain dehydrogenase reductase family. This enzyme might induce the enhanced degradation of prostaglandin E2 and promote $CD8^+$ T cell proliferation and interferon-γ production from T cells. Thus, it is possible that UBA1 and LTB4DH participate in the immune response against MTB.

TB is associated with oxidative stress and the induction of host antioxidants to counteract this response. In our study, 2 antioxidant enzymes, Prx-I and TKT, were identified in the plasma of individuals with LTBI. TKT serves as a reversible link between the oxidative branch of the pentose phosphate pathway and glycolysis, and it is a critical enzyme in the cellular defense against oxidative damage

(Lassen et al., 2008). We observed up-regulated expression of TKT, implying its important role as an antioxidant. Prx-I belongs to a ubiquitous peroxiredoxin family, which has been shown to have multiple functions, such as enhancing natural killer cell activity, increasing cell resistance to oxidative stress, regulating transcription activator protein, and protecting erythrocytes against oxidative stress (Chen et al., 2004). Our current data showed that the Prx-I level in LTBI individuals was lower than in healthy controls, suggesting that the capacity of self protection is impaired in LTBI individuals in response to oxidative stress. The presence of antioxidant enzymes in the plasma of LTBI individuals indicated that the antioxidative response has an important effect on MTB-induced oxidative injury.

In conclusion, the preliminary data in our study suggested that MALDI-TOF MS in combination with magnetic beads and bioinformatics tools was an effective technology for constructing diagnostic models. In particular, these powerful models could accurately differentiate healthy, latently infected individuals from healthy MTB-noninfected controls. However, the present study is a preliminary research; further studies, increasing the sample size and including other inflammatory diseases into control group, are needed to confirm these results and especially to subsequently validate the discovered proteins. Additionally, 14 potential LTBI biomarkers were identified. Some of the identified proteins might participate in the regulation of inflammatory, antioxidative and host immune responses against MTB. It should be noted that measuring plasma protein levels is technically much easier than other approaches, such as IGRA, and offers an economical and effective initial detection tool in a clinical setting. It is our hope that further validation of these plasmatic profiles in LTBI will provide information on LTBI-associated targets and the process of pathogenesis.

Supplementary data to this article can be found online at http://dx.doi.org/10.1016/j.diagmicrobio.2014.04.005.

Acknowledgments

This work was supported by the National Science and Technology Major Project of China (no. 2013ZX10003003 and 2012ZX10003002) and Beijing health systems of high-level health and technical personnel training plan (no. 2009-3-51).

References

Aichem A, Pelzer C, Lukasiak S, Kalveram B, Sheppard PW, Rani N, et al. USE1 is a bispecific conjugating enzyme for ubiquitin and FAT10, which FAT10ylates itself in cis. Nat Commun 2010;1:13.

Bandow JE, Baker JD, Berth M, Painter C, Sepulveda OJ, Clark KA, et al. Improved image analysis workflow for 2-D gels enables large-scale 2-D gel-based proteomics studies-COPD biomarker discovery study. Proteomics 2008;8:3030–41.

Baumann S, Ceglarek U, Fiedler GM, Lembcke J, Leichtle A, Thiery J. Standardized approach to proteome profiling of human serum based on magnetic bead separation and matrix-assisted laser desorption/ionization time-of-flight mass spectrometry. Clin Chem 2005;51:973–80.

Centers for Disease Control and Prevention (CDC). Targeted tuberculin testing and treatment of latent tuberculosis infection. American Thoracic Society. MMWR Recomm Rep 2000;49:1–51.

Chen JH, Chang YW, Yao CW, Chiueh TS, Huang SC, Chien KY, et al. Plasma proteome of severe acute respiratory syndrome analyzed by two-dimensional gel electrophoresis and mass spectrometry. Proc Natl Acad Sci U S A 2004;101:17039–44.

Cheng AJ, Chen LC, Chien KY, Chen YJ, Chang JT, Wang HM, et al. Oral cancer plasma tumor marker identified with bead-based affinity-fractionated proteomic technology. Clin Chem 2005;51:2236–44.

Chien JY, Jerng JS, Yu CJ, Yang PC. Low serum level of high-density lipoprotein cholesterol is a poor prognostic factor for severe sepsis. Crit Care Med 2005;33:1688–93.

Dekker LJ, Burgers PC, Charif H, van Rijswijk AL, Titulaer MK, Jenster G, et al. Differential expression of protease activity in serum samples of prostate carcinoma patients with metastases. Proteomics 2010;10:2348–58.

Deng C, Lin M, Hu C, Li Y, Gao Y, Cheng X, et al. Exploring serological classification tree model of active pulmonary tuberculosis by magnetic beads pretreatment and MALDI-TOF MS analysis. Scand J Immunol 2011;74:397–405.

Dye C, Scheele S, Dolin P, Pathania V, Raviglione MC. Consensus statement. Global burden of tuberculosis: estimated incidence, prevalence, and mortality by country. WHO Global Surveillance and Monitoring Project. JAMA 1999;282:677–86.

Endeman H, Meijvis SC, Rijkers GT, van Velzen-Blad H, van Moorsel CH, Grutters JC, et al. Systemic cytokine response in patients with community-acquired pneumonia. Eur Respir J 2011;37:1431–8.

Faulkner S, Elia G, Mullen MP, O'Boyle P, Dunn MJ, Morris D. A comparison of the bovine uterine and plasma proteome using iTRAQ proteomics. Proteomics 2012;12:2014–23.

Fertin M, Burdese J, Beseme O, Amouyel P, Bauters C, Pinet F. Strategy for purification and mass spectrometry identification of SELDI peaks corresponding to low-abundance plasma and serum proteins. J Proteomics 2011;74:420–30.

Fiedler GM, Leichtle AB, Kase J, Baumann S, Ceglarek U, Felix K, et al. Serum peptidome profiling revealed platelet factor 4 as a potential discriminating peptide associated with pancreatic cancer. Clin Cancer Res 2009;15:3812–9.

Huang Z, Shi Y, Cai B, Wang L, Wu Y, Ying B, et al. MALDI-TOF MS combined with magnetic beads for detecting serum protein biomarkers and establishment of boosting decision tree model for diagnosis of systemic lupus erythematosus. Rheumatology 2009;48:626–31.

Ishigami N, Tokuda T, Ikegawa M, Komori M, Kasai T, Kondo T, et al. Cerebrospinal fluid proteomic patterns discriminate Parkinson's disease and multiple system atrophy. Mov Disord 2012;27:851–7.

Jasmer RM, Nahid P, Hopewell PC. Clinical practice. Latent tuberculosis infection. N Engl J Med 2002;347:1860–6.

Komori M, Matsuyama Y, Nirasawa T, Thiele H, Becker M, Alexandrov T, et al. Proteomic pattern analysis discriminates among multiple sclerosis-related disorders. Ann Neurol 2012;71:614–23.

Lassen N, Black WJ, Estey T, Vasiliou V. The role of corneal crystallins in the cellular defense mechanisms against oxidative stress. Semin Cell Dev Biol 2008;19:100–12.

Lawn SD, Zumla AI. Tuberculosis. Lancet 2011;378:57–72.

Liu YW, Yang MH, Liu PY, Lee CH, Liao PC, Tyan YC. Proteomic analysis of pericardial effusion: characteristics of tuberculosis-related proteins. Proteomics Clin Appl 2008;2:458–66.

Lu C, Wu J, Wang H, Wang S, Diao N, Wang F, et al. Novel biomarkers distinguishing active tuberculosis from latent infection identified by gene expression profile of peripheral blood mononuclear cells. PLoS One 2011;6:e24290.

Martìnez Cordero E, Gonzàlez MM, Aguilar LD, Orozco EH, Hernàndez Pando R. Alpha-1-acid glycoprotein, its local production and immunopathological participation in experimental pulmonary tuberculosis. Tuberculosis (Edinb) 2008;88:203–11.

Menzies D. What does tuberculin reactivity after bacille Calmette-Guérin vaccination tell us? Clin Infect Dis Suppl 2000;3:S71–4.

Mikkat S, Koy C, Ulbrich M, Ringel B, Glocker MO. Mass spectrometric protein structure characterization reveals cause of migration differences of haptoglobin alpha chains in two-dimensional gel electrophoresis. Proteomics 2004;4:3921–32.

National Institute for Health and Clinical Excellence. Tuberculosis: clinical diagnosis and management of tuberculosis, and measures for its prevention and control; 2011 [Available at: http://guidance.nice.org.uk/CG117].

Pai M, Riley LW, Colford Jr JM. Interferon-gamma assays in the immunodiagnosis of tuberculosis: a systematic review. Lancet Infect Dis 2004;4:761–76.

Piñeiro M, Andrés M, Iturralde M, Carmona S, Hirvonen J, Pyörälä S, et al. ITIH4 (inter-alpha-trypsin inhibitor heavy chain 4) is a new acute-phase protein isolated from cattle during experimental infection. Infect Immun 2004;72:3777–82.

Sakamoto K, Geisel RE, Kim MJ, Wyatt BT, Sellers LB, Smiley ST, et al. Fibrinogen regulates the cytotoxicity of mycobacterial trehalose dimycolate but is not required for cell recruitment, cytokine response, or control of mycobacterial infection. Infect Immun 2010;78:1004–11.

Sandhu G, Battaglia F, Ely BK, Athanasakis D, Montoya R, Valencia T, et al. Discriminating active from latent tuberculosis in patients presenting to community clinics. PLoS One 2012;7:e38080.

Schwamborn K, Krieg RC, Grosse J, Reulen N, Weiskirchen R, Knuechel R, et al. Serum proteomic profiling in patients with bladder cancer. Eur Urol 2009;56:989–96.

Sester M, Sotgiu G, Lange C, Giehl C, Girardi E, Migliori GB, et al. Interferon-γ release assays for the diagnosis of active tuberculosis: a systematic review and meta-analysis. Eur Respir J 2011;37:100–11.

Shao L, Zhang W, Zhang S, Chen CY, Jiang W, Xu Y, et al. Potent immune responses of Ag-specific Vgamma2Vdelta2+ T cells and CD8+ T cells associated with latent stage of *Mycobacterium tuberculosis* coinfection in HIV-1-infected humans. AIDS 2008;22:2241–50.

Sterling TR, Bethel J, Goldberg S, Weinfurter P, Yun L, Horsburgh CR. The scope and impact of treatment of latent tuberculosis infection in the United States and Canada. Am J Respir Crit Care Med 2006;173:927–31.

Sterling TR, Villarino ME, Borisov AS, Shang N, Gordin F, Bliven-Sizemore E, et al. Three months of rifapentine and isoniazid for latent tuberculosis infection. N Engl J Med 2011;365:2155–66.

Tufariello JM, Chan J, Flynn JL. Latent tuberculosis: mechanisms of host and bacillus that contribute to persistent infection. Lancet Infect Dis 2003;3:578–90.

Wan J, Sun W, Li X, Ying W, Dai J, Kuai X, et al. Inflammation inhibitors were remarkably up-regulated in plasma of severe acute respiratory syndrome patients at progressive phase. Proteomics 2006;6:2886–94.

Wong MY, Yu KO, Poon TC, Ang IL, Law MK, Chan KY, et al. A magnetic bead-based serum proteomic fingerprinting method for parallel analytical analysis and micropreparative purification. Electrophoresis 2010;31:1721–30.

World Health Organization (WHO). Standard tuberculin test. WHO/TB/Technical Guide/85.145; 1963 [Geneva, Switzerland].